Journal of Electronics and Electrical Engineering
https://ojs.wiserpub.com/index.php/JEEE

Research Article

Filtering of Quasi Periodic Stochastic Systems Using Robust Techniques

Miguel A. Vázquez-Olguín[1], José A. Andrade-Lucio[1], Shunyi Zhao[2], Yuriy S. Shmaliy[1]*

[1] Department of Electronics Engineering, Universidad de Guanajuato, Salamanca 36855, Mexico
[2] The Key Laboratory of Advanced Process Control for Light Industry, Jiangnan University, Wuxi 214122, China
* Correspondence: shmaliy@ugto.mx

Received: 11 February 2026; **Revised:** 16 March 2026; **Accepted:** 30 March 2026; **Published:** 3 April 2026

Abstract: The behavior of a periodic system becomes quasi-periodic when it is driven by noise or operates under perturbations (disturbances and/or uncertainties). If the perturbation is not Gaussian, a robust state estimator is required. In this paper, we consider a quasi-periodic conservative Llinear Time Invariant (LTI) stochastic system driven by white Gaussian noise, the measurement of which is carried out in the presence of unknown but norm-bounded measurement disturbance. Therefore, choosing a proper estimator is a challenging task in each special case. Based on real data of daily quasi-periodic and hourly averaged measurements of nitrogen oxide NO_x contamination, the Kalman filter is shown to be the worst tracker of daily smoothed data. The best performance demonstrate the unbiased finite impulse response filter and the robust peak-to-peak $\mathscr{L}_1$ filter developed using the error-to-error transfer function (ERTF) approach. Other ERTF-based energy-to-peak GH_2 and energy-to-energy H_∞ filters provide in-between estimates.

Keywords: quasi-periodic disturbed system, transfer function approach, Unbiased Finite Impulse Response (UFIR) filter, $\mathscr{L}_1$ filter, GH_2 filter, H_∞ filter, Kalman Filter (KF)

1. Introduction

When a periodic system is driven by noise or operates under perturbations (disturbances and/or uncertainties), its behavior becomes quasi periodic [1]. Therefore, its supposedly periodic motion in fact never exactly duplicates itself, since the spectral content corresponding to periodic behavior is blurred by extraneous components. All physical periodic systems exhibit quasi-periodic behaviour due to natural noise sources [2, 3]. Even in the most accurate quantum oscillators, the frequency Power Spectral Density (PSD) has side branches around the fundamental frequency, which cannot always be ignored [4]. More examples follow. An electrocardiogram [5] is a process that is a recording of the heart's activity. Since the heartbeat rate depends on physical activity and heart health, the electrocardiogram is a quasi periodic process [6]. The periodic motion of planets around the Sun is actually quasi-periodic due to a number of factors influencing the dynamics of the motion [7], such as multiple, incommensurate frequencies (e.g., rotation, revolution, and orbital perturbations) [8]. The Gamma function is an almost periodic or quasi-periodic function because it acts as a continuous extension of the factorial function, displaying quasi-periodic behaviour due to this recurrent structure [9]. Quasiperiodicity is also characteristic of Gamma-ray astronomy [10].

The list of examples could be largely expanded, but we wish to focus on processes related to climate and air quality, which are attracting increasing attention in our modern life [11–13]. As is known, globalization and industrialization

DOI: https://doi.org/10.37256/jeee.5120269787

require an increase in human activity, which affects air quality at urban, regional, continental and global scales [14]. This has made air quality monitoring an indispensable process aimed at measuring and analyzing pollutants like ozone O_3, nitric oxide NO_x, nitrogen dioxide NO_2, sulfur dioxide SO_2, carbon monoxide CO, etc. [15]. Measurements are typically made here using complex sensor devices and networks, an example of which is an array of 5 metal oxide chemical sensors embedded in an Air Quality Chemical Multisensor Device [16]. The commonly accepted metric is the Air Quality Index (AQI) [17] that ranges within the interval 0-500 and is used to indicate health risks from pollutants: the low risk (0–50) is green and the high risk ($>$ 301) is maroon [18].

It is important to note that noise in quasi-periodic air quality processes is not necessarily Gaussian, and measurements may be accompanied by disturbances, uncertainties, outliers, and missing data. This makes conventional state estimators such as the Kalman Filter (KF) ineffective and requires robust solutions. In this regard, robust state estimators based on the error-to-error transfer function (ERTF) approach are considered to be the most effective [19, 20]. Over the past decades, the following robust ERTF-based filters have been developed using Linear Matrix Inequality (LMI). The H_∞ filtering problem formulated in [21] was subsequently developed in many works [22–25] based on the bounded real lemma. This filter minimized the $\mathscr{L}_2$ norm of the norm-bounded output error for the maximized $\mathscr{L}_2$ norm of the norm-bounded perturbations and hence guarantees the energy-to-energy performance. The generalized H_2 (GH_2) filtering problem was originally formulated in [26] and later developed in [27, 28] and other works [19, 29–31] into the $\mathscr{L}_2$-to-$\mathscr{L}_\infty$ filter and using the energy-to-peak lemma. This filter minimized the $\mathscr{L}_\infty$ norm of the norm-bounded output error for the maximized $\mathscr{L}_2$ norm of the norm-bounded perturbations and guarantees the energy-to-peak performance. In some cases, a process is affected by unknown but norm-bounded impulsive disturbances [32], and an estimator may react with overshot errors [33]. To deal with it, the $\mathscr{L}_1$ filtering problem originally discussed in [34] through the convolution, was later solved in many works [35–41] using the peak-to-peak lemma. This filter minimized the $\mathscr{L}_\infty$ norm of the norm-bounded output error for the maximized $\mathscr{L}_\infty$ norm of the norm-bounded perturbations, thereby ensuring peak-to-peak performance. Setting aside the ERTF approach, the robust Unbiased Finite Impulse Response (UFIR) filter was proposed in [42] and then widely used by many authors as having potentially the best robustness amidst other state estimators [43].

In this paper, we examine the performance of different filtering algorithms applied to a typical quasi periodic process associated with air pollution data. We compare the robust H_∞, GH_2, $\mathscr{L}_1$, and UFIR filters as well as the KF in terms of Root Mean Square Error (RMSE), robustness, and estimation quality. Base upon, we conclude that no filtering method can guarantee the best estimate in the presence of highly distorted and time-varying data, and that proper tuning and accurate knowledge of noise and perturbation statistics play a crucial rule here. The main contributions are as follows:

• Forward Euler method-based state space model of a quasi-periodic process and the corresponding system noise covariance.

• Advanced robust H_∞, GH_2, and $\mathscr{L}_1$ filtering algorithms for which the bias correction gain is computed numerically using LMI.

• Experimental evidence that for daily averaging of measurements of nitrogen oxide NO_x quasi-periodic concentration, the robust $\mathscr{L}_1$ and UFIR filters provide the smallest Root Mean Square (RMS) and peak errors.

The remaining part of the paper is organized as follows. Section 2 discusses the quasi-periodic system and formulates the problem. Section 3 introduces the robust ERTF-based $\mathscr{L}_1$, GH_2, and H_∞ filters, ad well as the UFIR and Kalman filters. In Section 4, we conduct experimental testing of the filtering algorithms based on hourly averaged measurement of nitrogen oxides NO_x concentration in a highly polluted city area. Finally, conclusions are drawn in Section 5.

2. Model and problem formulation

As follows from Section 1, many physical processes are quasi periodic by nature, and we list some of them in Table 1. Taking into account their quasi periodicity and stationarity, many of them can be represented by a Llinear Time Invariant (LTI) conservative stochastic system of the second order $\ddot{u}(t)+\omega_0^2 u(t)=w(t)$, where ω_0 is the angular fundamental frequency and $w(t)\sim\mathscr{N}(0,\mathscr{C}_w)$ is white Gaussian noise with the covariance $\mathrm{cov}(w)=E\{w(t)w(t+\tau)\}=\mathscr{C}_w\delta(\tau)$, where

$\delta(\tau)$ is the Dirac delta and $\mathscr{C}_w = \frac{N_w}{2}$ is the uniform power spectral density (PSD) of noise $w(t)$. Added the measurement noise $v(t)$, this equation can be represented in state space as follows [19]:

$$\dot{x}(t) = Ax(t) + Lw(t), \tag{1}$$

$$y(t) = Cx(t) + v(t), \tag{2}$$

where $x(t)$ is the state vector, the matrices are given by

$$A = \begin{bmatrix} 0 & 1 \\ -\omega_0^2 & 0 \end{bmatrix}, \quad L = \begin{bmatrix} 0 \\ 1 \end{bmatrix}, \quad C = \begin{bmatrix} 1 & 0 \end{bmatrix}, \tag{3}$$

and $v(t) \sim \mathscr{N}(0, \mathscr{C}_v)$ is the measurement noise with the covariance $\text{cov}(v) = E\{v(t)v(t+\tau)\} = \frac{N_v}{2}\delta(\tau)$, where $\mathscr{C}_v = \frac{N_v}{2}$ is the uniform PSD of the measurement noise $v(t)$.

Table 1. Examples of quasi periodic processes

	Quasi Periodic Process
Air Quality	Concentration of ozone O_3, nitric oxide NO_x, nitrogen dioxide NO_2, carbon monoxide CO, etc. [15].
Medicine	Electrocardiogram of heartbeat rate, depending on physical activity and heart health [6].
Engineering	Quantum oscillations, whose frequency PSD has side branches around the fundamental frequency [4].
Cosmology	The motion of the planets around the Sun, influenced by rotation, revolution, and orbital perturbations [8].

Using the forward Euler method, the model (1) and (2) can be represented in discrete-time state-space as follows:

$$x_{k+1} = Fx_k + w_k, \tag{4}$$

$$y_k = Hx_k + v_k, \tag{5}$$

where k is the discrete tile index and $H = C$. The Cayley-Hamilton theorem applied to the matrix exponential $F = e^{A\tau}$ gives [19]

$$F = \begin{bmatrix} \cos\omega_0\tau & \frac{1}{\omega_0}\sin\omega_0\tau \\ -\omega_0\sin\omega_0\tau & \cos\omega_0\tau \end{bmatrix}, \tag{6}$$

where $\tau = t_k - t_{k-1}$ is the discrete-time step. The system noise $w_k \sim \mathscr{N}(0, Q)$ is defined by [19]

$$w_k = \int_{t_{k-1}}^{t_k} e^{A(t_k-\theta)} Lw(t)d\theta \tag{7}$$

to have the covariance, whose derivation is given in Appendix A,

$$Q = \frac{N_w \tau}{4} \begin{bmatrix} \omega_0^{-2}\left(1 - \frac{\sin 2\omega_0\tau}{2\omega_0\tau}\right) & \tau\left(\frac{\sin\omega_0\tau}{\omega_0\tau}\right)^2 \\ \tau\left(\frac{\sin\omega_0\tau}{\omega_0\tau}\right)^2 & 1 + \frac{\sin 2\omega_0\tau}{2\omega_0\tau} \end{bmatrix}. \tag{8}$$

Note that in the special case when τ is sufficiently small and hence $\frac{\sin x}{x} \approx 1 - \frac{x^2}{3!}$, the covariance (8) can be substituted with

$$Q \approx \frac{N_w \tau}{4} \begin{bmatrix} \frac{2\tau^2}{3} & \tau - \frac{\omega_0^2\tau^3}{3} \\ \tau - \frac{\omega_0^2\tau^3}{3} & 2 - \frac{2\omega_0^2\tau^2}{3} \end{bmatrix}. \tag{9}$$

The measurement noise $v_k \sim \mathcal{N}(0, R)$ is defined by

$$v_k = \frac{1}{\tau}\int_{t_{k-1}}^{t_k} v(\theta)d\theta \tag{10}$$

to have the covariance $\mathrm{cov}(v) = E\{v_k v_l\} = R\delta_{k-l}$, where $R = \sigma_v^2 = \frac{N_v}{2\tau}$ and δ_n is the Kronecker delta. Recall that accurate knowledge of the noise statistics is crucial to obtain the best estimation performance.

The problem can now be formulated as follows. Considering air quality processes as quasi-periodic processes represented by the model (4) and (5), we would like to apply the robust H_∞, GH_2, $\mathscr{L}_1$, and UFIR filters as well as the KF to real measurement data of the nitric oxide NO_x concentration in a heavily polluted urban area and compare their performances in terms of Root Mean Square Error (RMSE), robustness, and estimation quality.

3. Filtering algorithms

The following filtering algorithms will be applied to quasi-periodic air quality data represented by the LTI model (4) and (5): robust ERTF-based H_∞, GH_2, and $\mathscr{L}_1$ filters, UFIR filter, and KF. For reader, who are not away of the key features of these algorithms, we list advantages and disadvantages in Table 2. It is worth noting that filtering performance is highly dependent on operating conditions and modeling errors, and that selecting a suitable filter is often a challenging task. Therefore, experimental verification plays an important role.

Table 2. Key features of filtering algorithms related to quasi periodic stationary processes

	Advantages and disadvantages
H_∞ filter	Advantage: guarantees the robust energy-to-energy performance. Disadvantage: does not cope with peak errors and outliers.
GH_2 filter	Advantage: guarantees the robust energy-to-peak performance. Disadvantage: loses to H_∞ filter in the absence of impulsive perturbations.
$\mathscr{L}_1$ filter	Advantage: guarantees the robust peak-to-peak performance. Disadvantage: loses to H_∞ and GH_2 filters in the absence of impulsive perturbations.
UFIR filter	Advantage: does not require information about initial values and noise covariances. Disadvantage: is not an optimal state estimator.

Table 2. Cont.

	Advantages and disadvantages
Kalman filter	Advantage: guarantees the minimum MSE. Disadvantage: is not a robust state estimator.

3.1 *Robust ERTF-based filtering algorithms*

Since the robust ERTF-based filters minimize the error-to-error transfer function, their recursive a posteriori filtering estimate $\hat{x}_k \triangleq \hat{x}_{k|k}$ is given by [20]

$$\hat{x}_k = F\hat{x}_{k-1} + K(y_k - HF\hat{x}_{k-1}), \tag{11}$$

where the bias correction gain K is defined in different sense to satisfy the energy-to-energy, energy-to-peak, or peak-to-peak criterion. There are several ways of how to compute numerically K using the corresponding lemmas. One way is to represent the a posteriori estimation error ε_k in state space as

$$\varepsilon_{k+1} = F_\xi \varepsilon_k + B_\xi \xi_k, \tag{12}$$

$$r_k = H_\xi \varepsilon_k, \tag{13}$$

where the vector and matrices are defined by

$$\xi_k = \begin{bmatrix} w_k \\ v_{k+1} \end{bmatrix}, \quad Q_\xi = \begin{bmatrix} Q & 0 \\ 0 & R \end{bmatrix}, \quad F_\xi = (I - KH)F, \quad B_\xi = \begin{bmatrix} I - KH & -K \end{bmatrix}, \quad H_\xi = I. \tag{14}$$

Next, set the initial K and X to a proper lemma and solve an LMI for the a posteriori estimation error covariance P. Then solve for K the Lyapunov equation

$$P = (I - KH)FPF^T(I - KH)^T + (I - KH)Q(I - KH)^T + KRK^T, \tag{15}$$

and repeat this calculus iteratively until γ reaches a minimum. Finally run the recursive form (11). Since the core of this approach is the corresponding lemmas applied to the error model (12) and (13), we present them below, noting that the sign $\succ$ means positive definiteness and $\prec$ means negative definiteness.

3.1.1 *Bounded real lemma for H_∞ filtering [44]*

Given a discrete time stable system $\left[\begin{array}{c|c} F & B \\ \hline H & D \end{array}\right]$ represented in state-space using the forward Euler method by the following equations:

$$x_{k+1} = Fx_k + Bw_k, \tag{16}$$

$$y_k = Hx_k + Dw_k. \tag{17}$$

Let $\gamma > 0$, if there exists an invertible matrix $X \succ 0$ such that the following LMI is soluble,

$$\begin{bmatrix} -X & 0 & F^T & H^T \\ 0 & -\gamma^2 Q_\xi^{-1} & B^T & D^T \\ F & B & -X^{-1} & 0 \\ H & D & 0 & -P^{-1} \end{bmatrix} \prec 0, \tag{18}$$

then the following inequality

$$\frac{\sum_{i=m}^{k} y_i^T P y_i}{\sum_{i=m}^{k} w_i^T Q_\xi^{-1} w_i} < \gamma^2 \tag{19}$$

holds to guarantee the energy-to-energy H_∞ performance.

3.1.2 *Energy-to-peak lemma for GH_2 filtering [27]*

Given a discrete time stable system $\left[\begin{array}{c|c} F & B \\ \hline H & D \end{array}\right]$ represented in state-space by the equations (16) and (17). Let $\gamma > 0$ be a scalar, w_k be a bounded input $\|w_k\|^2_{P_w^{-1}} = w_k^T Q_\xi^{-1} w_k < \infty$, and y_k have a bounded weighted peak norm $\|y\|^2_{\infty P} < \infty$. The energy-to-peak $\mathscr{L}_2 - \mathscr{L}_\infty$ filtering performance is guaranteed by obeying

$$\sup_{0<\|w\|_2<\infty} \frac{\|y\|^2_{\infty P}}{\|w\|^2_{Q_\xi^{-1}}} < \gamma^2, \tag{20}$$

if there exists an invertible matrix $X \succ 0$ such that

$$\begin{bmatrix} \gamma^2 P^{-1} - DD^T & H \\ H^T & X \end{bmatrix} \succ 0, \tag{21}$$

$$\begin{bmatrix} BQ_\xi B^T - X^{-1} & F \\ F^T & -X \end{bmatrix} \prec 0. \tag{22}$$

3.1.3 *Peak-to-peak lemma for $\mathscr{L}_1$ filtering [19, 45, 46]*

Given a discrete time stable system $\left[\begin{array}{c|c} F & B \\ \hline H & D \end{array}\right]$ represented in state space using the forward Euler method by the equations (16) and (17). Let $\gamma > 0$ be a small real scalar, $0 < \mu < \lambda < 1$ be real scalars, $\alpha = 1 - \lambda$, $\beta = 1 - \frac{\mu}{\lambda} > 0$, and w_k be a bounded disturbance, $\|w\|_\infty < \infty$. The $\mathscr{L}_\infty$–$\mathscr{L}_\infty$ performance is guaranteed by satisfying the condition

$$\sup_{0<\|w\|_\infty<\infty} \frac{\|y\|^2_{\infty P}}{\|w\|^2_{\infty Q_\xi^{-1}}} < \gamma^2, \tag{23}$$

if there exists an invertible matrix $X \succ 0$ such that

$$\begin{bmatrix} -\alpha X & 0 & F^T \\ 0 & -\mu Q_\xi^{-1} & B^T \\ F & B & -X^{-1} \end{bmatrix} \prec 0, \tag{24}$$

$$\begin{bmatrix} X & 0 & H^T \\ 0 & \beta Q_\xi^{-1} & D^T \\ H & D & \gamma^2 P^{-1} \end{bmatrix} \succ 0. \tag{25}$$

3.2 *Robust UFIR filtering algorithms*

The a posteriori UFIR filtering algorithm operates iteratively on the horizon of N data points, from $m = k-N+1$ to K, and minimizes RMSE when N is set optimally as N_{opt}. A pseudo code of this algorithm is listed as Algorithm 1 in Appendix B. To get started, it only needs the data y_k, an auxiliary partitioned matrix $C_K = \begin{bmatrix} (HF^{-K+1})^T & \dots & (HF^{-1})^T & H^T \end{bmatrix}^T$, and the initial Generalized Noise Power Gain (GNPG) matrix $\mathscr{G}_s = (C_K^T C_K)^{-1}$. It then iteratively updates the a posteriori estimate $\hat{x}_k$ from $s+1$ to k. Since this algorithm ignores the zero-mean noise statistics and the initial values, it is considered the most robust among all other linear filters. Note that for a given averaging horizon of N points, the UFIR filter becomes blind—a property that is highly required in many applications.

3.3 *Kalman filtering algorithm*

A pseudo code of the conventional a posteriori KF algorithm is listed as Algorithm 2 in Appendix C. This algorithm is optimal for mutually uncorrelated white Gaussian noise sequences w_k and v_k given initial values $\hat{x}_0$ and P_0 and precisely known noise covariances Q and R. Otherwise, violation of these condition may severely degrade its performance. Therefore, the KF is considered a non-robust estimator.

4. Experimental testing

To test different filtering techniques, we have chosen hourly averaged measurement of the nitric oxide NO_x represented by the nominally targeted sensor response and available from [47]. The NO_x process is quasi periodic, and our goal is to obtain the best filtering estimates of daily smoothed raw data. This makes the filtering task exceedingly heavy, since the variations of hourly averaged data relative to daily smoothed data are extremely far from white Gaussian noise.

First, we convert the sensor data scale to parts per billion (ppb) using data obtained from a reference analyzer. To apply filters, we use the model (4) and (5) with $\tau = 1$, $f_0 = \frac{1}{24\tau}$, $\omega_0 = 2\pi f_0$, $H = \begin{bmatrix} 1 & 0 \end{bmatrix}$, and matrix F given by (6). To compensate for the phase shift, we replace $w_0\tau$ with $w_0\tau - 0.075\pi$ in the matrix F. Next, we run the UFIR filtering Algorithm 1 on a daily horizon of 24 points and then apply UFIR smoothing to obtain a smoothed estimate $\hat{x}_{k-q|k} = F^{-q}\hat{x}_{k|k}$ with lag $q = 12$ from the UFIR filtering estimate $\hat{x}_{k|k}$. The hourly averaged raw NO_x data and the smoothed data are exhibited in Figure 1 over a period of 20 days. In what follows, we will consider the smoothed behaviour as a Pseudo Ground Truth (PGT).

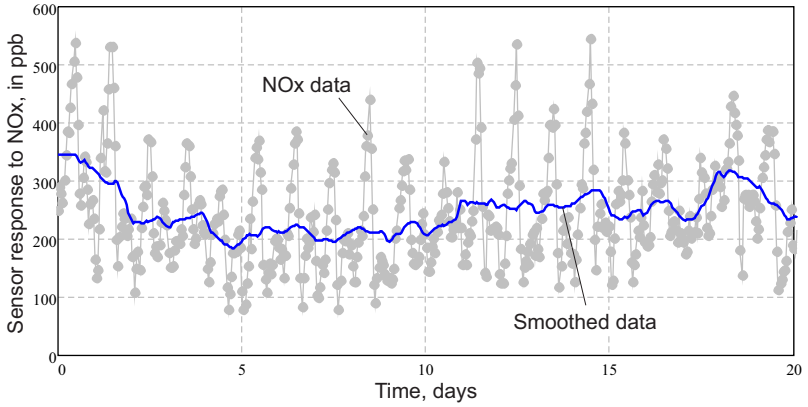

Figure 1. Hourly averaged raw measurements (NO_x data) of total nitrogen oxides (NO_x) in a highly polluted city area [47] and data obtained by an UFIR smoother (Smoothed data) with a 12-hour lag on an averaging horizon of 24 hours

To tune the KF, we use a part of measurement of 80 days and call it basic. For this database, we average the second state (velocity) available from the PGT, accept the error of 20% in the velocity determination, and based upon assign the standard deviation of the second state noise $\sigma_w = 3.8$ ppb/sec. For the measurement noise sequence $v_k \sim \mathcal{N}(0, \sigma_v^2)$, we experimentally set $\sigma_v = 69$ ppb taken from the database. Next, we set the initial values of $\hat{x}_0 = \text{PGT}_0$ and $P_0 = \text{diag}\,(\,\sigma_v^2 \;\; \sigma_v^2\,)$ and numerically compute the gains for the H_∞, GH_2, and $\mathscr{L}_1$ filters using the above described ERTF-based algorithms, for the KF after all transients are over, and for the UFIR filter at the end of the optimal averaging horizon of $N_{\text{opt}} = 36$ points. The gains computed are listed in Table 3, from which we see that K of the H_∞ filter has the maximum $\|K\|_1$ norm, the UFIR filter has the minimum norm, and the remaining filter have in-between norms. This means that the gains of the ERTF-based filters obey the rule of thumb recently formulated in [20].

Table 3. Performances of the $\mathscr{L}_1$, H_∞, $\mathscr{L}_2$-to-$\mathscr{L}_\infty$, Kalman, and UFIR filters applied to NO_x concentration measurements. The Best Values are Bolded

	UFIR	$\mathscr{L}_1$	GH_2	Kalman	H_∞
Gain K	$\begin{bmatrix}0.1417\\0.0542\end{bmatrix}$	$\begin{bmatrix}0.2135\\0.1441\end{bmatrix}$	$\begin{bmatrix}0.3681\\0.3892\end{bmatrix}$	$\begin{bmatrix}0.3685\\0.3929\end{bmatrix}$	$\begin{bmatrix}0.4970\\0.6007\end{bmatrix}$
$\|K\|_1$	0.1959	0.3576	0.7573	0.7614	1.0977
RMSE (base)	**64.4139**	71.1691	87.3136	87.5899	97.0673
RMSE (R1)	46.1025	**45.2186**	52.8923	49.4135	61.2567
RMSE (R2)	**53.3742**	59.3949	72.4307	69.2158	78.6668
RMSE (R3)	**82.5522**	85.2932	98.1383	102.0103	103.6217
Peak error (base)	118.2332	**98.5541**	180.4027	180.8098	223.4713
Peak error (R1)	**109.884**	115.7332	154.3152	142.8518	182.2939
Peak error (R2)	101.0538	**97.252**	144.463	132.2642	162.4508
Peak error (R3)	**198.6409**	262.5244	332.3091	337.9933	337.6278
Robustness ρ (R1)	**0.7157**	0.6354	0.6058	0.5641	0.6311
Robustness ρ (R2)	0.8286	**0.8346**	0.8295	0.7902	0.8104
Robustness ρ (R3)	0.7184	0.8015	0.876	0.8354	**0.9325**
Quality factor, ν (R1)	**0.0111**	0.0089	0.0069	0.0064	0.0065
Quality factor, ν (R2)	**0.0129**	0.0117	0.0095	0.0090	0.0083
Quality factor, ν (R3)	0.0112	**0.0113**	0.0100	0.0095	0.0096

The filtering estimates and estimation errors in the first and second states are sketched in Figure 2. As we can see, the filters do not approach PGT (bold) equally: the UFIR and $\mathscr{L}_1$ filters look the best, while the H_∞ and Kalman filters definitely give the worst estimates. This does not take by surprise since the UFIR filter ignores zero-mean perturbations, and the $\mathscr{L}_1$ filter minimizes peak errors for maximized peak perturbations. To strengthen these findings and generalize the results, we next normalize the errors in each of the four realizations by dividing them by the corresponding errors of the $\mathscr{L}_1$ filter. This makes the $\mathscr{L}_1$ filter normalized errors equal to one, and all other errors take values around this level. The corresponding normalized bar charts are shown in Figure 3, and we infer that the $\mathscr{L}_1$ filter generally outperforms all other filters except the UFIR one. It wins over other filters in terms of RMSE in 81.25% cases, in terms of peak errors in the first state in 87.5% cases, and in terms of peak errors in the second state in 68.75% cases. A bit better efficiency demonstrates only the UFIR filter.

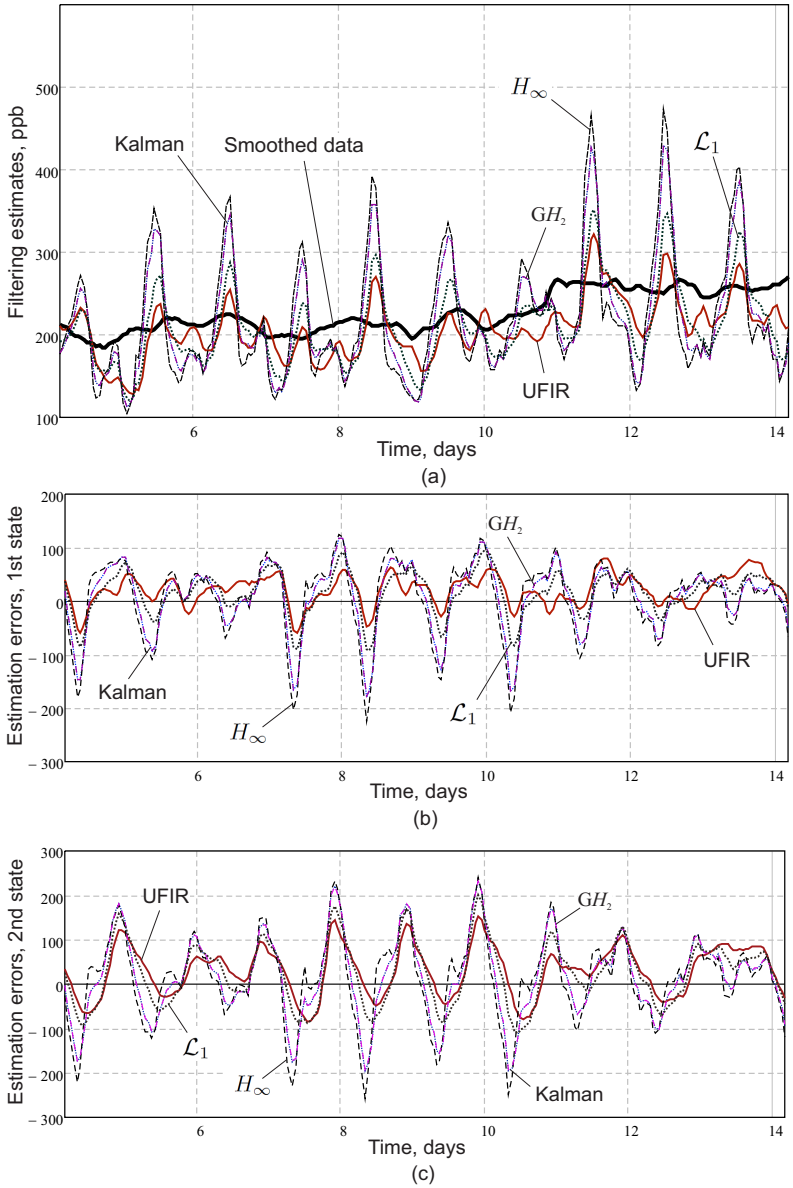

Figure 2. Filtering estimates and estimation errors produced by the $\mathscr{L}_1$, GH_2, H_∞, Kalman, and UFIR filters, relative to PGT (Smoothed data): (a) filtering estimates, (b) estimation errors in the first state, and (c) estimation errors in the second state

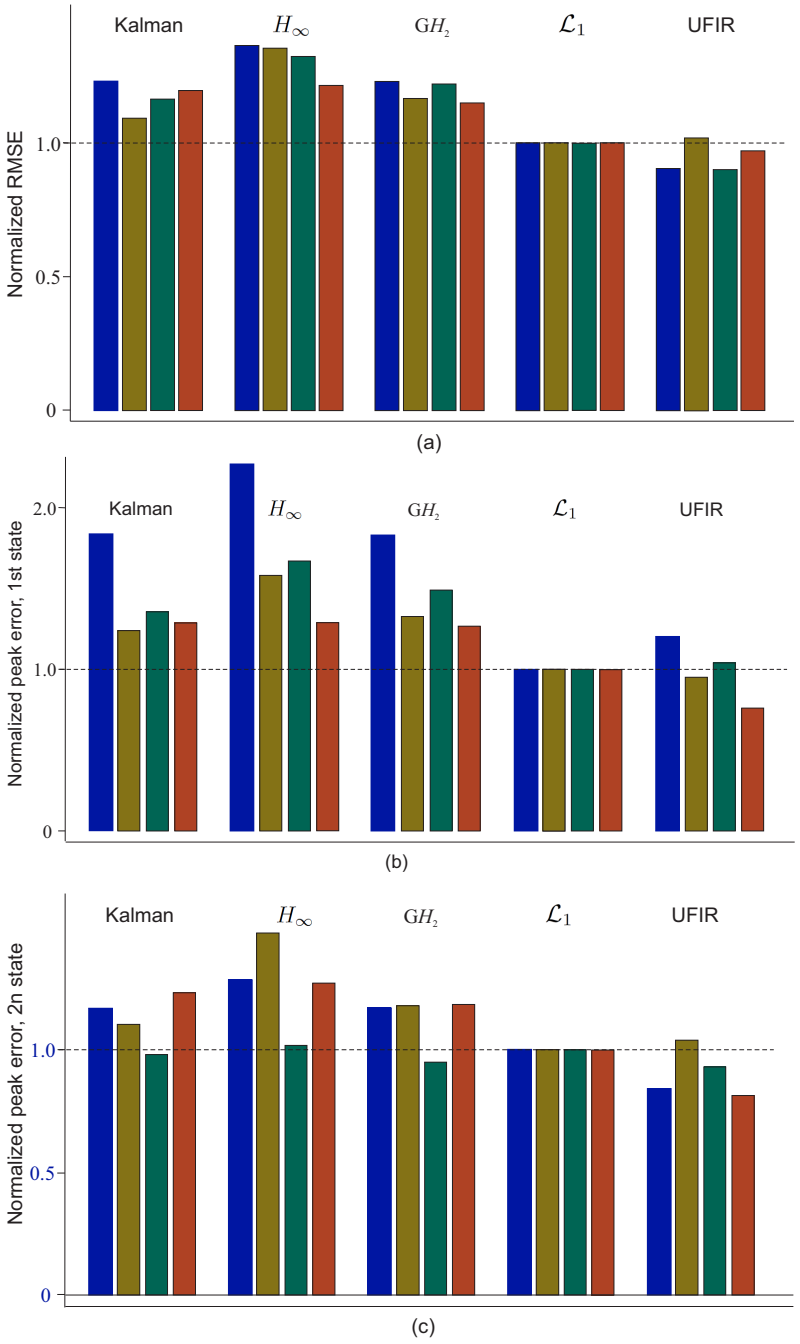

Figure 3. Normalized bar chats of the estimation errors produced by the $\mathscr{L}_1$, GH_2, H_∞, Kalman, and UFIR filters using four non-overlapping realizations of the same measurement database of hourly averaged NO_x concentration: (a) RMSEs, (b) peak errors in the first state, and (b) peak errors in the second state. The errors are normalized with respect to the $\mathscr{L}_1$ filter

To test the filters for robustness, we retain the baseline data setup and apply filtering to three other non-overlapping 80-days realizations of the same measurements, labeled as R1, R2, and R3. Then we compute the errors and put then into Table 3. Following the definition given by Huber [48] and using the formula proposed in [20], we compute the robustness factor ρ by

$$\rho(\mathrm{R}) = 1 - \frac{|\mathrm{RMSE(base)} - \mathrm{RMSE(R)}|}{\mathrm{RMSE(base)}}. \tag{26}$$

where $\mathrm{R} \in \{\mathrm{R1}, \mathrm{R2}, \mathrm{R3}\}$, and the Estimation Quality Factor (EQF) ν defined in [20] by

$$\nu(\mathrm{R}) = \frac{\rho(\mathrm{R})}{\mathrm{RMSE(base)}}. \tag{27}$$

This rounds off the idea of the filter performance. From Table 3, it follows that the UFIR filter is the most robust for R1 with $\rho = 0.7157$, the $\mathscr{L}_1$ filter is the most robust for R2 with $\rho = 0.8346$, and the H_∞ filter is the most robust for R3 with $\rho = 0.9325$. It can also be seen that the UFIR filter demonstrates the largest EQF for R1 with $\nu = 0.0111$ and for R2 with $\nu = 0.0129$, while the $\mathscr{L}_1$ filter has the largest EQF of $\nu = 0.0113$ for R3.

To summarize, it can be said the UFIR and $\mathscr{L}_1$ filters provide a better solution to the smoothing problem over 24-days for the considered database, while the other filters, as a rule, are inferior in terms of estimation errors, robustness and EQF.

5. Conclusions

Quasi periodicity is inherent to many physical processes, i.e. processes associated with daily changes in air quality, heartbeat rate, physical and biological vibrations and oscillations, planetary motion, etc. Since such processes are often subject to noise, disturbances, and perturbations, and are modeled under uncertainties, robust estimators are needed to estimate their states. Since filtering performance is highly dependent on operating conditions and modeling errors, selecting a suitable filter is often a challenging task. Therefore, experimental verification plays an important role in each special case.

Testing of ERTF-based robust $\mathscr{L}_1$, GH_2 and H_∞ filters, as well as the UFIR and Kalman filters by real measurements of the quasi-periodic and hourly averaged behavior of nitrogen oxide NO_x concentration in heavily polluted urban area have shown the following. With respect to daily smoothed data, the best estimates give the UFIR and $\mathscr{L}_1$ filters, while the Kalman filter gives the worst estimates. Other ERTF-based GH_2 and H_∞ filters provide in-between estimates. The UFIR and $\mathscr{L}_1$ filters have proved to be the most robust estimators with the largest EQF. They provide the best solution to the 24-hours smoothing problem, while other filters generally perform worse in terms of estimation errors, robustness, and EQF.

It is worth noting that the filters may not necessarily show the same results for other databases and conditions. To develop a practical guide for the user, we are currently working with other archives and plan to report the results in the near future.

Appendix A. Derivation of the system noise covariance

Consider the system noise w_k defined by (7). To find the covariance for w_k, first transform the integral form (7) as follows:

$$w_k = \int_{t_{k-1}}^{t_k} \begin{bmatrix} \cos\omega_0(t_k-\theta) & \frac{1}{\omega_0}\sin\omega_0(t_k-\theta) \\ -\omega_0\sin\omega_0(t_k-\theta) & \cos\omega_0(t_k-\theta) \end{bmatrix} \begin{bmatrix} 0 \\ 1 \end{bmatrix} w(t)d\theta$$

$$= \int_{t_{k-1}}^{t_k} \begin{bmatrix} \omega_0 \sin \omega_0 (t_k - \theta) \\ \omega_0^2 \cos \omega_0 (t_k - \theta) \end{bmatrix} w(t) d\theta \,. \tag{A1}$$

Next, consider the covariance $\mathrm{cov}(w_k) = E\{w_k w_l\} = Q\delta_{k-l}$, refer to (A1), and write $E\{w_k w_l\}$ as

$$E\{w_k w_l\} = \int_{t_{k-1}}^{t_k} \int_{t_{k-1}}^{t_k} \begin{bmatrix} \omega_0 \sin \omega_0 (t_k - \theta_1) \\ \omega_0^2 \cos \omega_0 (t_k - \theta_1) \end{bmatrix} E\{w(\theta_1) w(\theta_2)\} \begin{bmatrix} \omega_0 \sin \omega_0 (t_k - \theta_2) \\ \omega_0^2 \cos \omega_0 (t_k - \theta_2) \end{bmatrix}^T d\theta_1 d\theta_2$$

$$= \frac{N_w}{2} \int_{t_{k-1}}^{t_k} \int_{t_{k-1}}^{t_k} \delta(\theta_2 - \theta_1) \begin{bmatrix} \omega_0 \sin \omega_0 (t_k - \theta_1) \\ \omega_0^2 \cos \omega_0 (t_k - \theta_1) \end{bmatrix} \begin{bmatrix} \omega_0 \sin \omega_0 (t_k - \theta_2) \\ \omega_0^2 \cos \omega_0 (t_k - \theta_2) \end{bmatrix}^T d\theta_1 d\theta_2$$

$$= \frac{N_w}{2} \int_{t_{k-1}}^{t_k} \begin{bmatrix} \omega_0^2 \sin^2 \omega_0 (t_k - \theta) & \frac{\omega_0^3}{2} \sin 2\omega_0 (t_k - \theta) \\ \frac{\omega_0^3}{2} \sin 2\omega_0 (t_k - \theta) & \omega_0^4 \cos^2 \omega_0 (t_k - \theta) \end{bmatrix} d\theta \,. \tag{A2}$$

Finally, use the integral identities $\int \sin^2 ax\, dx = \frac{x}{2} - \frac{1}{4a} \sin 2ax + C$, $\int \sin ax\, dx = -\frac{1}{a} \cos ax + C$, and $\int \cos^2 ax\, dx = \frac{x}{2} + \frac{1}{4a} \sin 2ax + C$, provide the integration, and arrive at the closed form (8).

Appendix B. UFIR filtering algorithm

Algorithm 1 The *a posteriori* UFIR filtering algorithm

Input: y_k
Output: $\hat{x}_k$
  for $k = K, K+1, \cdots$ **do**
    $m \leftarrow \begin{cases} 0, & k \leqslant N-1 \\ k-N+1, & k > N-1 \end{cases}$
    $s \leftarrow m + K - 1$
    $Y_{m,s} \leftarrow \begin{bmatrix} y_m^T & y_{m+1}^T & \cdots & y_s^T \end{bmatrix}^T$
    $\hat{x}_s \leftarrow \mathscr{G}_s C_K^T Y_{m,s}$
    for $i = s+1 : k$ **do**
      $\breve{x}_i^- \leftarrow F \breve{x}_{i-1}$
      $\mathscr{G}_i \leftarrow [H^T H + (F \mathscr{G}_{i-1} F^T)^{-1}]^{-1}$
      $K_i \leftarrow \mathscr{G}_i T^T$
      $\breve{x}_i \leftarrow \breve{x}_i^- + K_i (y_i - T \breve{x}_i^-)$
    end for
    $\hat{x}_k \leftarrow \breve{x}_k$
  end for

Appendix C. Kalman filtering algorithm

Algorithm 2 The *a posteriori* KF Algorithm

Input: $y_k, \hat{x}_0, P_0, Q, R$
Output: $\hat{x}_k, P_k$
  for $k = 1, 2, \cdots$ **do**
    $\hat{x}_k^- \leftarrow F\hat{x}_{k-1}$
    $P_k^- \leftarrow FP_{k-1}F^T + Q$
    $S_k \leftarrow HP_k^- H^T + R$
    $K_k \leftarrow P_k^- H^T S_k^{-1}$
    $\hat{x}_k \leftarrow \hat{x}_k^- + K_k(y_k - H\hat{x}_k^-)$
    $P_k \leftarrow (I - K_k T)P_k^-$
  end for

Conflicts of interest

The authors declare no conflicts of interest.

References

[1] H. W. Broer, G. B. Huitema, and M. B. Sevryuk, *Quasi-Periodic Motions and Families of Dynamical Systems: Order Amidst Chaos*. Berlin, Germany: Springer-Verlag, 1996. https://doi.org/10.1007/978-3-540-49613-7.

[2] W. Wang, J. Chen, P. Tian, L. C. Ho, X. Sun, P. Wang, et al., "Quasi-periodic oscillations of GHz-band polarization in a black hole," *Nature Communications*, vol. 16, no. 5139, pp. 1-10, 2025. https://doi.org/10.1038/s41467-025-59586-5.

[3] D. Kong, X. Sun, L. Zhang, Y. Hu, and J. Duan, "Superhydrophobic quasi-periodic concave microlens array on fused silica prepared by spatially modulated picosecond laser parallel processing," *Ceramics International*, vol. 50, no. 21-B, pp. 42922-42932, 2024. https://doi.org/10.1016/j.ceramint.2024.08.138.

[4] Y. S. Shmaliy, *GPS-based Optimal FIR Filtering of Clock Models*. New York, NY, USA: Nova Science Publishers, 2009.

[5] J. P. Varshney, *Electrocardiography in Veterinary Medicine*. Singapore: Springer Nature, 2020. https://doi.org/10.1007/978-981-15-3699-1.

[6] B. Bernhard, A. Brensing, and K.-H. Witte, *Biosignal Processing: Fundamentals and Recent Applications with MATLAB*. Berlin, Germany: Walter de Gruyter GmbH, 2022. https://doi.org/10.1515/9783110736298.

[7] A. Celletti and S. Ferraz-Mello, *Periodic, Quasi-Periodic and Chaotic Motions in Celestial Mechanics: Theory and Applications*. Dordrecht, The Netherlands: Springer, 2006. https://doi.org/10.1007/978-1-4020-5325-2.

[8] J. Fitzgerald and S. D. Ross, "Geometry of transit orbits in the periodically-perturbed restricted three-body problem," *Advances in Space Research*, vol. 70, no. 1, pp. 144-156, 2022. https://doi.org/10.1016/j.asr.2022.04.029.

[9] P. H. Bezandry and T. Diagana, *Almost Periodic Stochastic Processes*. New York, NY, USA: Springer, 2011. https://doi.org/10.1007/978-1-4419-9476-9.

[10] V. Guedes, D. Radice, C. Chirenti, and K. Yagi, "Tight bound on the neutron star radius with quasiperiodic oscillations in short gamma-ray bursts," *The Astrophysical Journal*, vol. 983, no. 2, pp. 1-9, 2025. https://doi.org/10.3847/1538-4357/adc101.

[11] V. M. Sharma and S. Jain, "Unmanned aerial vehicles and low-cost sensors for air quality monitoring: a comprehensive review of applications across diverse emission sources," *Sustainable Cities and Society*, vol. 127, 2025. https://doi.org/10.1016/j.scs.2025.106409.

[12] G. Silva, J. Duarte, J. S. Baptista, and J. C. Rufo, "Low-cost sensors for indoor air quality monitoring: a systematic review of accuracy, applications, and limitations," *Journal of the Air & Waste Management Association*, pp. 1-27, 2026. https://doi.org/10.1080/10962247.2026.2624795.

[13] A. I. Mirza, J. H. Kazmi, S. Shaikh, and N. S. Arshad, "Monitoring urban air quality in lahore: a combined approach using ground measurements and sentinel 5P data," *International Journal of Environmental Science and Technology*, vol. 23, no. 207, 2026. https://doi.org/10.1007/s13762-025-06976-3.

[14] B. R. Gurjar, L. T. Molina, and S. S. P. Ojha, Eds., *Air Pollution: Health and Environmental Impacts*. Boca Raton, FL, USA: CRC Press, 2010.

[15] World Health Organization, *Air Quality Guidelines: Global Update 2005*. Copenhagen, Denmark: World Health Organization, 2006.

[16] S. De Vito, E. Massera, M. Piga, L. Martinotto, and G. Di Francia, "On field calibration of an electronic nose for benzene estimation in an urban pollution monitoring scenario," *Sensors and Actuators B: Chemical*, vol. 129, no. 2, pp. 750-757, 2008. https://doi.org/10.1016/j.snb.2007.09.060.

[17] E. Elabd, H. M. Hamouda, M. A. Mohamed Ali, A. S. Hamid, and Y. Fouad, "Air quality index AQI classification based on hybrid particle swarm and grey wolf optimization with ensemble machine learning model," *Scientific Reports*, vol. 16, pp. 1-21, 2026. https://doi.org/10.1038/s41598-025-34278-8.

[18] R. H. Friis, *Essentials of Environmental Health*. Burlington, MA, USA: Jones & Bartlett Learning, 2019.

[19] Y. S. Shmaliy and S. Zhao, *Optimal and Robust State Estimation: Finite Impulse Response (FIR) and Kalman Approaches*. New York, NY, USA: John Wiley & Sons, 2022. https://doi.org/10.1002/9781119863106.

[20] O. G. Ibarra-Manzano, J. A. Andrade-Lucio, M. A. Vazquez-Olguin, and Y. S. Shmaliy, "Transfer function-based robust filtering: review and critical evaluation," *Signal Processing*, vol. 237, pp. 1-13, 2025. https://doi.org/10.1016/j.sigpro.2025.110060.

[21] B. Hassibi, A. H. Sayed, and T. Kailath, *Indefinite-Quadratic Estimation and Control: A Unified Approach to H_2 and H_∞ Theories*. Philadelphia, PA, USA: SIAM, 1999. https://doi.org/10.1137/1.9781611970760.

[22] F. L. Lewis, L. Xie, and D. Popa, *Optimal and Robust Estimation with an Introduction to Stochastic Control Theory*. Boca Raton, FL, USA: CRC Press, 2008. https://doi.org/10.1201/9781315221656.

[23] M. D. Nisar, *Minimax Robustness in Signal Processing for Communications*. Aachen, Germany: Shaker Verlag, 2011.

[24] O. G. Ibarra-Manzano, J. A. Andrade-Lucio, Y. Xu, and Y. S. Shmaliy, "Bias correction gain for recursive H_∞-Kalman filtering of non-predictive uncertain models," *IEEE Signal Processing Letters*, vol. 32, pp. 871-875, 2025. https://doi.org/10.1109/LSP.2025.3539576.

[25] J. A. Andrade-Lucio, O. G. Ibarra-Manzano, M. A. Vázquez-Olguín, and Y. S. Shmaliy, "Recursive H_∞ filtering: computing gain using LMI for backward Euler method-based disturbed models," *Journal of the Franklin Institute*, vol. 363, no. 3, 2026. https://doi.org/10.1016/j.jfranklin.2026.108406.

[26] D. A. Wilson, "Convolution and Hankel operator norms for linear systems," *IEEE Transactions on Automatic Control*, vol. 34, no. 1, pp. 94-97, 1989. https://doi.org/10.1109/9.8655.

[27] R. E. Skelton, T. Iwasaki, and K. M. Grigoriadis, *A Unified Algebraic Approach to Linear Control Design*. London, U.K.: Taylor & Francis, 1998.

[28] J. T. Watson and K. M. Grigoriadis, "Optimal unbiased filtering via linear matrix inequalities," *Systems & Control Letters*, vol. 35, no. 2, pp. 111-118, 1998. https://doi.org/10.1016/S0167-6911(98)00042-5.

[29] H. Gao and X. Li, *Robust Filtering for Uncertain Systems: A Parameter-Dependent Approach*. New York, NY, USA: Springer, 2014. https://doi.org/10.1007/978-3-319-05903-7.

[30] J. H. Park, H. Shen, X.-H. Chang, and T. H. Lee, *Recent Advances in Control and Filtering of Dynamic Systems with Constrained Signals*. New York, NY, USA: Springer, 2019. https://doi.org/10.1007/978-3-319-96202-3.

[31] L. Cao, X. Chen, and B. Xiao, *Predictive Filtering for Microsatellite Control System*. Cambridge, MA, USA: Academic Press, 2021. https://doi.org/10.1016/C2019-0-04217-3.

[32] K. Wang, P. Wu, B. Zhao, L. Kong, and S. He, "Reconstructed variational Bayesian Kalman filter under heavy-tailed and skewed noises," *IEEE Signal Processing Letters*, vol. 31, pp. 2405-2409, 2024. https://doi.org/10.1109/LSP.2024.3453189.

[33] Y. Tao and S. Shing-Toung Yau, "Outlier-robust iterative extended Kalman filtering," *IEEE Signal Processing Letters*, vol. 30, pp. 743-747, 2023. https://doi.org/10.1109/LSP.2023.3285118.

[34] M. Vidyasagar, "Optimal rejection of persistent bounded disturbances," *IEEE Transactions on Automatic Control*, vol. 31, no. 6, pp. 527-534, 1986. https://doi.org/10.1109/TAC.1986.1104315.

[35] Y. Ohta and Y. Toude, “Minimization of the maximum peak-to-peak gain with time domain constraints on fixed input response,” In Proc. the 38th IEEE Conference on Decision and Control, Phoenix, AZ, USA, Dec. 7-10, 1999, pp. 1439-1444. https://doi.org/10.1109/CDC.1999.830179.

[36] S. Chen, N. Cao, W. Zhang, and B. Yu, “Separation of aliasing signals from inductive oil debris monitors based on fully convolutional neural networks,” *Measurement Science and Technology*, vol. 33, no. 11, 2022. https://doi.org/10.1088/1361-6501/ac7f1c.

[37] J. V. Salcedo, M. Martínez, S. G. Rodriguez, and A. Hilario, “BIBO stabilisation of continuous-time Takagi – Sugeno systems under persistent perturbations and input saturation,” *International Journal of Applied Mathematics and Computer Science*, vol. 28, no. 3, pp. 457-472, 2018. https://doi.org/10.2478/amcs-2018-0035.

[38] X.-H. Chang, J. Wang, and X. Zhao, “Peak-to-peak filtering for discrete-time singular systems,” *IEEE Transactions on Circuits and Systems II: Express Briefs*, vol. 68, no. 7, pp. 2543-2547, 2021. https://doi.org/10.1109/TCSII.2021.3049840.

[39] J. Song and X.-H. Chang, “Finite-time peak-to-peak filtering for nonlinear singular system,” *IEEE Transactions on Circuits and Systems II: Express Briefs*, vol. 69, no. 11, pp. 4369-4373, 2022. https://doi.org/10.1109/TCSII.2022.3179249.

[40] N. Nafie, A. El-amrani, N. Chaibi, and B. Boukili, “Robust filtering design for periodic piecewise polytopic systems over a low-frequency range,” *Procedia Computer Science*, vol. 274, pp. 835-844, 2025. https://doi.org/10.1016/j.procs.2025.12.082.

[41] E. Gershon and U. Shaked *Advanced Topics in Control and Estimation of State-Multiplicative Noisy Systems*. London, U.K.: Springer, 2013. https://doi.org/10.1007/978-1-4471-5070-1.

[42] Y. S. Shmaliy, “An iterative Kalman-like algorithm ignoring noise and initial conditions,” *IEEE Transactions on Signal Processing*, vol. 59, no. 6, pp. 2465-2473, 2011. https://doi.org/10.1109/TSP.2011.2129516.

[43] S. Zhao, J. Wang, Y. S. Shmaliy, and F. Liu, “Discrete time *q*-lag maximum likelihood FIR smoothing and iterative recursive algorithm,” *IEEE Transactions on Signal Processing*, vol. 69, no. 2, pp. 6342-6354, 2021. https://doi.org/10.1109/TSP.2021.3127677.

[44] S. Boyd, L. El Ghaoui, E. Feron, and V. Balakrishnan, *Linear Matrix Inequalities in System and Control Theory*. Philadelphia, PA, USA: SIAM, 1994. https://doi.org/10.1137/1.9781611970777.

[45] J. Abedor, K. Nagpal, and K. Poola, “A linear matrix inequality approach to peak-to-peak gain minimization,” *International Journal of Robust and Nonlinear Control*, vol. 6, no. 9-10, pp. 899-927, 1996. https://doi.org/10.1002/(SICI)1099-1239(199611)6:9/10<899::AID-RNC259>3.0.CO;2-G.

[46] T. Vincent, J. Abedor, K. Nagpal, and P. P. Khargonekar, “Discrete-time estimators with guaranteed peak-to-peak performance,” *IFAC Proceedings Volumes*, vol. 29, no. 1, pp. 4470-4475, 1996. https://doi.org/10.1016/S1474-6670(17)58385-8.

[47] UCI Machine Learning Repository, “Air quality,” 2016. [Online]. Available: https://doi.org/10.24432/C59K5F. [Accessed Feb. 10, 2026].

[48] P. J. Huber, *Robust Statistics*. New York, NY, USA: John Wiley & Sons, 1981. https://doi.org/10.1002/0471725250.